



**HAL**  
open science

## Bunch Extension Monitor for LINAC of SPIRAL2 facility

R. Revenko, J.L. Vignet

► **To cite this version:**

R. Revenko, J.L. Vignet. Bunch Extension Monitor for LINAC of SPIRAL2 facility. 2nd International Beam Instrumentation Conference - IBIC2013, Sep 2013, Oxford, United Kingdom. pp.720-722, 2013. in2p3-00864194

**HAL Id: in2p3-00864194**

**<https://hal.in2p3.fr/in2p3-00864194>**

Submitted on 11 Mar 2014

**HAL** is a multi-disciplinary open access archive for the deposit and dissemination of scientific research documents, whether they are published or not. The documents may come from teaching and research institutions in France or abroad, or from public or private research centers.

L'archive ouverte pluridisciplinaire **HAL**, est destinée au dépôt et à la diffusion de documents scientifiques de niveau recherche, publiés ou non, émanant des établissements d'enseignement et de recherche français ou étrangers, des laboratoires publics ou privés.

# BUNCH EXTENSION MONITOR FOR LINAC OF SPIRAL2 FACILITY

R. Revenko, J. L. Vignet, GANIL, Caen, France

## Abstract

Measurements of the bunch longitudinal shape of beam particles are crucial for optimization and control of the LINAC beam parameters and maximization of its integrated luminosity. The non-interceptive bunch extension monitor for LINAC of SPIRAL2 facility is being developed at GANIL. The five bunch extension monitors are to be installed on the entrance of LINAC between superconducting cavities. The principle of monitor operation is based on registration of x-rays induced by ions of accelerator beam and emitted from thin tungsten wire. The monitor consists of two parts: system for wire insertion and positioning and x-ray detector based on microchannel plates. The prototype of detector has been developed and was tested using protons and heavy ions beams.

## INTRODUCTION

The SPIRAL2 project [1] is based on a multi-beam LINAC driver in order to allow both ISOL and low-energy in-flight techniques to produce RIB. A superconducting light/heavy-ion LINAC with an acceleration potential of about 40 MV capable of accelerating 5 mA deuterons up to 40 MeV and 1 mA heavy ions up to 14.5 MeV/u is used to bombard both thick and thin targets. These beams could be used for the production of intense RIB by several reaction mechanisms (fusion, fission, transfer, etc.) and technical methods (ISOL, IGISOL, recoil spectrometers, etc.). The production of high intensity RIB of neutron-rich nuclei will be based on fission of uranium target induced by neutrons, obtained from a deuteron beam impinging on a graphite converter (up to  $10^{14}$  fissions/s) or by a direct irradiation with a deuteron,  $^3\text{He}$  or  $^4\text{He}$  beam.

The accelerating RF of LINAC [2] is 88,0525 MHz. It means that time distance between two bunches is 11,26 ns. The extension of the phase for bunch ( $\pm 2\sigma$ ) is  $60^\circ$  or  $\sim 1,6$  ns for bunch length. The LINAC can operate at continuous or pulsed mode with period of macropulse varied at range from 100  $\mu\text{sec}$  to 1 sec.

Correct adjustment of LINAC is necessary conditions for obtaining maximal intensity and luminosity on the target. Adjusting includes synchronization of phase for each acceleration section. For this reason information about spatial beam particles distribution is needed. While the beam transverse profile will be measured by pick up monitors (BPM) information about bunch longitudinal distribution will be obtained by bunch extension monitor (BEM). These diagnostic detectors will be placed in gaps between superconducting acceleration cavities inside the warm sections. Each warm section consists of two quadrupoles and diagnostic box between them. Five BEM will be mounted into first five diagnostic boxes on entrance of LINAC.

## BEM DESCRIPTION

Bunch extension monitor is a non-destructive beam diagnostic detector for estimation of longitude of LINAC bunches. Principle of operation of BEM based on registration of x-rays emitted from thin tungsten wire due to interaction it with ions beam. Comparing to monitors based on secondary emission of electrons there is not applied potential on the wire and thus it is not produce distortion of the beam optics. The LINAC will be operated at vacuum level  $10^{-8}$  mbar thus all components of BEM should meet to UHV requirements. All materials of BEM components must satisfy required conditions of purity for preventing of cavity pollution.

### BEM Working Principle

The photons emitted from the wire will be produced due to ionization of atoms by hitting of ions beam. The ions can knock-out electrons from inner shells and produce electron vacancy. Electrons from outer shells fill this vacancy and emit the difference of energy of bound states as characteristic x-ray photons. The energies of emitted characteristic photon are unique for each element and in case of tungsten they are 60 keV and 11 keV for K- and L-shell ionization respectively. Due to interaction of x-rays with material of MCP they produce photoelectrons which than multiplied at two stages of MCP. The MCP has a very fast response time with signal of few hundred mV and rise time 700-800 picoseconds. Output signal is transmitted thru coaxial cable on input of constant fraction discriminator CFD 7174. Signal of accelerator RF comes to another channel of CFD. Two logical signals from CFD output as "start" and "stop" signals feed time-to-amplitude converter Ortec 566. The time difference between two logical signals is measured. Output signal from TAC with amplitude proportional to time difference is digitized by multichannel analyzer Ortec 921. The principal schema of BEM electronics operation is presented in Fig. 1.

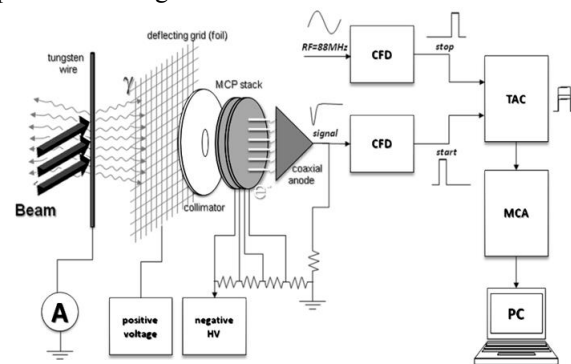


Figure 1: Principal schema of operation of BEM electronics.

Gamma source of  $^{55}\text{Fe}$  with was used for estimation of temporal resolution for electronics. Output signal from prototype of x-ray detector was transmitted thru the long coaxial cable 74 meters length and then splitted on two signal by splitter. After splitter signals were going in input of CFD with one of signal was previously delayed for 10ns. Measured time resolution for electronics was  $\text{FWHM}=33\pm 3.2\text{ps}$ .

**BEM Design**

The BEM constructively consist of two parts which are installed inside the one diagnostic box and occupied two flanges CF100 (see Fig.2).

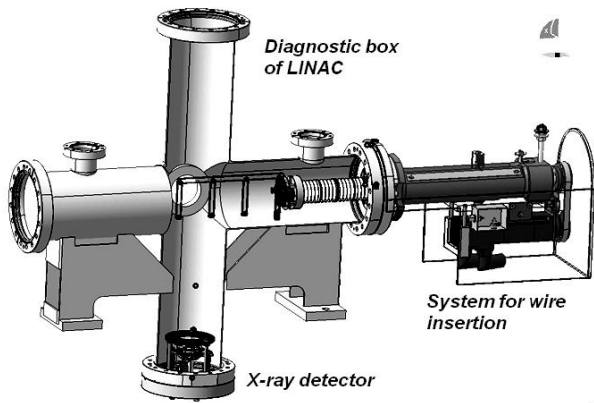


Figure 2: General view of BEM installed at diagnostic box of LINAC.

The first part is system for wire insertion which allows inserting the wire into the beam and making their positioning with precision less than 100  $\mu\text{m}$ . Tungsten wires 150 microns diameter are fixed on stainless steel frame inside of three holders. Each holder has dimensions 50 mm  $\times$  50 mm where tungsten wire is fixed at diagonally across. Wires of the next BEM are fixed in their holders at perpendicular direction to the wires of previous BEM for minimization of influence one detector to another and on LINAC beam. The three positions of wires allow replacing on wire to another in case of damaging one without disassembling all mechanism. The frame with wire holders is connected thru isolator with rod of linear actuator which has a length of the moving 178mm. The rod is moved by brushless motor thru the system of screw-nut. The brushless motor is a part of the Siemens SIMATIC 110 which also includes power supply and control module. Motor and mechanical parts of actuator are mounted on air side of flange CF100.

The system for wire insertion allows performing measurements of current pick up from the wire. Frame with fixed on it tungsten wires is electrically connected thru vacuum feedthrough with BNC connector on the flange. Current from the wire is measured by card of chassis for current measurements which was developed at GANIL by GEM group and also used for measurements of current from FC and slits.

The second part of BEM is x-ray detector used for registration of photons emitted from wire and it is based on MCP design. Detector is placed at distance 240mm from the wire. There is being used microchannel plates Hamamatsu F1551 ( $\varnothing$  18mm) with channel diameter 12 $\mu\text{m}$ . The two MCP are assembled at chevron configuration and provide summary gain up to  $10^8$  at applied voltage  $-2$  kV. The MCP has electrodes covered by Inconel alloy. For providing of short front of signal the output electrons are collected by fast readout coaxial anode which are matched on 50 Ohms impedance and connected with N-type connector on the flange CF100. Entrance of first MCP is covered by copper collimator which has hole  $\varnothing$  4mm and thickness 8 mm and provides registration of photons at solid angle  $2 \times 10^{-4}\text{sr}$ .

To escape background signals from ions coming from residual gas ionization at the front of detector is mounted deflecting grid and positive potential +30V is applied on it. All electronic components of HV divider a placed inside a box and located on the air side of diagnostic box.

**TEST OF PROTOTYPE**

The first test of BEM prototype was performed at proton beam of IPN'O tandem accelerator. Measurements were done at energies 4, 10 and 18 MeV. This test approved the principle of operation of this detector. High value of background events were measured during this test. Background events were case registration of ions from residual gas ionization due to the bad vacuum condition ( $10^{-5}$  mbar instead  $10^{-8}$  mbar)

As improvement the deflecting grid was added to design of BEM prototype. The second test was performed at GANIL with beam of  $^{36}\text{Ar}^{+10}$  ions with energy 0,98 MeV/n. Measurements were done at different values of intensity and applied voltage on MCP. The results of the test were shown increasing of values measured bunch length with increasing of applied high voltage on MCP that can be explained by effect of saturation. The optimal value of HV was chosen at  $-1,95$  kV (see Fig. 3).

One more test at high intensities beam is needed for estimation of dynamic range of detector.

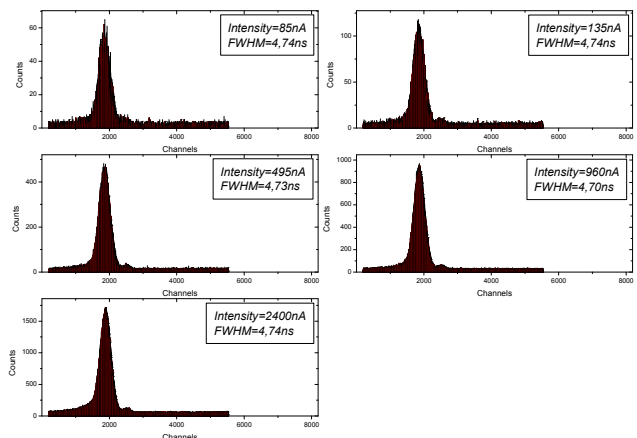


Figure 3: Measured bunch profile of  $^{36}\text{Ar}^{+18}$  beam at different intensities. Value of applied voltage is  $-1.95\text{kV}$ .

### Comparison with Theoretical Estimation

Results of the test were compared with analytical calculation of x-ray production from the wire (see Fig 4). To perform these calculations a cross section of tungsten wire was divided into small elemental cells. For each cell was calculated a value of ionization cross section of atoms material the wire. The cross-section can be implemented as a function of scaled velocity of projectile ion to velocity of electron on the shell  $V_{proj}/V_{elect}$  and can be represented thru Gryzinsky function (see Eq.1) [3].

$$\sigma_{ionis}(E) = \frac{N \cdot Z^2 \cdot \sigma_0}{U^2} \cdot G(V) \quad (1)$$

Where  $N$  is a number of electrons on the shell (K-shell=2, L-shell=8),  $Z$  is charge of projectile ion,  $U$  is binding energy of electrons at the given shell,  $G(V)$  is a function of the scaled velocity  $V = V_{proj}/V_{elect}$  and  $\sigma_0 = \pi \cdot e_0 = 6.56 \times 10^{-14} \text{ cm}^2 eV^2$ .

To estimate scaled velocity the value of  $dE/dx$  for beam energy is calculated in each cell. Also attenuation of x-rays emitted at direction of x-ray detector is taken in account by material.

The total value of emitted photon from the wire can be obtained by summing x-ray production in each cell of wire cross-section [4]. The final expression for total numbers of photons emitted in solid angle  $d\Omega/4\pi$  and registered by MCP can be written as:

$$Q = \frac{\Omega}{4\pi} \cdot \varepsilon \cdot N_{atoms} \cdot \omega_{k,l} \cdot \sum_{ij} I_{ij} \cdot \sigma_{ionis}(E(x_i)) \cdot e^{-\mu \cdot L_{ij}} \quad (2)$$

where  $d\Omega/4\pi$  is a solid angle of detector,  $\varepsilon$  is a efficiency of registration photons by MCP,  $N_{atoms}$  is concentration of target atoms per  $\text{cm}^2$ ,  $\omega_{k,l}$  is fluorescence yields of photons for K-, L-shell ionizations,  $I_{ij}$  is number of incident ions of the beam at  $ij$ -cell per second,  $\sigma_{ionis}$  is ionization cross-section for K-,L-shells as function of incident ion energy,  $exp(-\mu \cdot L_{ij})$  is attenuation of x-ray at material of target.

The calculations (see Eq. 2) were done for both case of ionization for K- and L- shell. The relative yield of photons due to ionization of L-shell is at almost  $10^5$  times more than one for K-shell. For this reason in comparison with experimental results mainly are using values of calculations for L-shell.

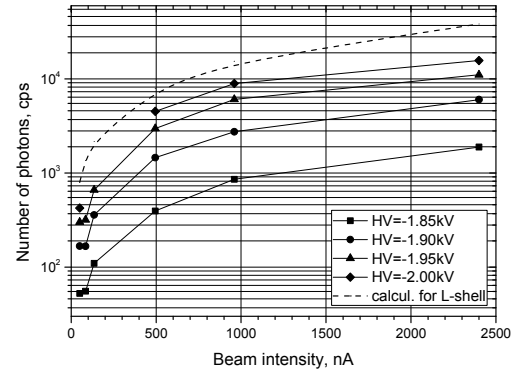


Figure 4: Comparison of count rates for different values intensities and applied voltage. Theoretical estimation of count rate due L-shell ionisation is presented.

### SUMMARY

The prototype of non-interceptive beam diagnostic detector for bunch length measurements was developed. Test at proton and ions beams were performed at different conditions. The temporal resolution for detector electronics was measured and is  $33 \pm 3.2$  ps for analog electronics. The results of test were compared with theoretical estimation of x-ray production. The effect of saturation is observed and test with high intensity beam is needed. For estimation of background conditions test BEM will be performed at proximity of superconducting cavity.

### ACKNOWLEDGMENT

This work is funded in frame of CRISP WP3T1 project.

### REFERENCES

- [1] <http://www.ganil-spiral2.eu/>
- [2] D. Uriot et al., "Configuration de base du LINAC supraconducteur de SPIRAL2 V2.0", Référence Spiral 2 I-013103/1 (2008).
- [3] Michal Gryzinski, "Classical Theory of Atomic Collisions. I. Theory of Inelastic Collisions", Phys.Rev. V.138, 2A (1965) p.336
- [4] I. Orlic et al., "TPIXAN - A Package of computer programs for quantitative thick target PIXE analysis", NIM B49 (1990) p166.